Journal of Molecular Catalysis B: Enzymatic 66 (2010) 81–89

Contents lists available at ScienceDirect

Journal of Molecular Catalysis B: Enzymatic

journal homepage: www.elsevier.com/locate/molcatb

A novel thermophilic lipase from *Fervidobacterium nodosum* Rt17-B1 representing a new subfamily of bacterial lipases

Shanshan Yu[a], Songcheng Yu[a], Weiwei Han[a], Honglei Wang[a], Baisong Zheng[a], Yan Feng[a,b,*]

[a] *Key Laboratory for Molecular Enzymology and Engineering of Ministry of Education, Jilin University, Changchun 130023, China*
[b] *Key Laboratory of Microbial Metabolism (Ministry of Education) and College of Life Science and Biotechnology, Shanghai Jiao Tong University, Shanghai 200240, China*

ARTICLE INFO

Article history:
Received 29 November 2009
Received in revised form 14 March 2010
Accepted 15 March 2010
Available online 23 March 2010

Keywords:
Fervidobacterium nodosum Rt17-B1
Lipase
Phylogenetic analysis
Thermostability

ABSTRACT

Thermophilic enzymes have significant potential for industry applications due to their high inherent stability and high reaction rates at high temperatures. In this study a gene coding for a putative lipase composed of 302 amino acids from an anaerobic thermophilic bacterium *Fervidobacterium nodosum* Rt17-B1 was cloned and characterized. Phylogenetic analysis suggests that this novel lipase represents a new subfamily of family I of bacterial lipases, annotated as family I.8. The recombinant protein can catalyze the hydrolysis of *p*-nitrophenyl esters and shows substrate preference for *p*-nitrophenyl caprate with a k_{cat}/K_m of 22,500 s^{-1} μM^{-1}. Most importantly, it can hydrolyze triacylglycerols with long acyl chains. In the test conditions applied here it has a maximum activity at 70 °C and pH 9.0 and displays extreme thermal stability. Interestingly, it was not only stable, but was also activated by treatment with polar organic solvents including propanol, acetone, dimethyl sulfoxide (DMSO) and N,N-dimethylformamide (DMF). Structural modeling showed that it is composed of an α/β-hydrolase fold and a lid domain comprised of four α-helices. A canonical catalytic triad consisting of Ser119, Asp206 and His282 was verified by site-directed mutagenesis.

1. Introduction

Lipases have received a great deal of attention for their applicability in numerous industrial processes, including oils, fat leather and paper processing, baking, cheese making, cleaning hard-surfaces and as components of detergents [1]. The number of known bacterial lipases has increased considerably since the 1980s, and these enzymes have been grouped into eight families, based on differences in their amino acid sequences and fundamental biological properties [2]. Most lipases are members of family I, which catalyze the hydrolysis and synthesis of long-chain, poorly water-soluble substrates [3], and are classified into seven subfamilies. Structural analyses have revealed that they are composed of an α/β hydrolase fold and a "lid" domain which shields the active site [4]. Most of these enzymes contain a catalytic triad consisting of a nucleophilic serine located in a highly conserved Gly-X-Ser-X-Gly pentapeptide, and an aspartate residue that is hydrogen-bonded to a histidine [5]. Exceptions are lipases from thermophiles which contain the catalytic residue Ser located in an Ala-X-Ser-X-Gly sequence [6–12]. The enzymes of family I have also marked variations in enzyme properties, such as activity, stability and substrate spectra [2]. Thus, investigation of lipases in these organisms may both lead to the discovery of novel lipases and increase our knowledge of the diversity of lipases.

Furthermore, thermophiles are valuable sources of thermostable enzymes with properties that are often associated with stability in solvents and detergents, conferring to these enzymes considerable potential for many biotechnological and industrial applications. Several lipases from thermophiles have been characterized [13]. Based on the classification of bacterial lipases presented by Arpigny and Jaeger, all reported lipases from aerobic thermophilic bacteria, such as *Bacillus thermocatenulatus* I [6], *B. stearothermophilus* L1 [7], *G. thermoleovorans* ID-1 [8], *G. stearothermophilus* P1 [9], *G. thermoleovorans* Toshki [10], *Geobacillus* sp. T1 [11] and *G. thermoleovorans* CCR11 [12], belong to subfamily 5 of family I. The sequence similarities between these lipases exceed 90%, but they show some differences in properties with respect to temperature activity and stability. These thermophilic lipases have been found to have optimum temperatures between 55 and 70 °C. Lipase from *G. thermoleovorans* Toshki, which may retain 30% residual activity when incubated for 1 h at 100 °C [10], was

* Corresponding author at: Key Laboratory of Microbial Metabolism (Ministry of Education) and College of Life Science and Biotechnology, Shanghai Jiao Tong University, 800 Dong-Chuan Road, Shanghai 200240, China. Tel.: +86 21 34207189; fax: +86 21 34207189.
E-mail addresses: yfeng2009@mail.sjtu.edu.cn, yfeng@mail.jlu.edu.cn (Y. Feng).

1381-1177/$ – see front matter © 2010 Elsevier B.V. All rights reserved.
doi:10.1016/j.molcatb.2010.03.007

the most thermophilic lipase of family I.5 that had been examined at that time. Other members of the family have been found to be stable between 40 and 60 °C, but unable to withstand temperatures exceeding 70 °C [6–9,11,12]. In terms of substrate specificity, these lipases show preferences for *p*-nitrophenyl esters and triacylglycerols with medium to long-chain fatty acids, except the lipase from *B. thermocatenulatus* which has high activity toward tributyrin (C_4) [6]. In addition to these thermophilic lipases of aerobic thermophilic origins, two themophilic lipases from an anaerobic thermophilic bacterium, *Thermosyntropha lipolytica*, have been described initially by Wiegel and coworker [14]. These lipases are the most thermophilic reported to date since they retained 50% activity following incubation at 100 °C up to 6 h. However, they have not been classified into any bacterial lipase family because their cognate genes were not reported. Hence, knowledge about the lipases from thermophiles is limited compared to that of their mesophilic counterparts. However, industrial demands for enzymes with desirable properties continue to stimulate attempts to discover and characterize novel lipases from thermophiles.

Fervidobacterium nodosum Rt17-B1 is an anaerobic thermophilic bacterium of the eubacterial order Thermotogales, which includes the most extremely thermophilic eubacteria currently known and represents the deepest phylogenetic branch within the bacteria. It is capable of growing at temperatures substantially exceeding 60 °C, with an optimum of about 80 °C [15]. Several genes encoding putative esterase/lipases have been annotated in its genome, but none of them have been previously characterized. In order to obtain potentially useful thermophilic lipases from *F. nodosum* Rt17-B1, we cloned, purified and characterized a novel bacterial lipase (FnL). We then demonstrated that FnL represent a new subfamily of family I of bacterial lipases. As the first detected member of this new subfamily, FnL was characterized in terms of catalytic properties such as substrate profiles, stability and kinetic behavior, and effects of mutations of the conservative catalytic triad. Furthermore, structural modeling was conducted to analyze the interactions between the enzyme and substrates in the active site.

2. Materials and methods

2.1. Strains and materials

Strain *F. nodosum* Rt17-B1 was purchased from DSMZ and grown aerobically at 65 °C (15). The media contained per litre of distilled water: NH_4Cl, 0.9 g; $MgCl_2$, 0.2 g; KH_2PO_4, 0.75 g; K_2HPO_4, 1.5 g; trace mineral solution, 9 ml; 10% $FeSO_4$, 0.03 ml; 0.2% resazurin, 1 ml; 5 ml of vitamin solution; yeast extract, 3 g; trypticase peptone, 10 g and glucose 5 g. Trace mineral solution contained per litre distilled water: 12.5 g nitrilotriacetic acid neutralized to pH 6.5 with KOH; $FeCl_3{\cdot}4H_2O$, 0.2 g; $MnCl_2{\cdot}H_2O$, 0.1 g; $CoCl_2{\cdot}6H_2O$, 0.017 g; $CaCl_2{\cdot}2H_2O$, 0.1 g; $ZnCl_2$, 0.1 g; $CuCl_2$, 0.02 g; H_3BO_3, 0.01 g; $NaMoO_4{\cdot}2H_2O$, 0.01 g; NaCl, 1.0 g and Na_2SeO_3, 0.02 g. A steady stream of O_2-free nitrogen gas was allowed to flow through the inlet of the dispenser via a bent syringe needle as the media cooled. 10 ml of 10% $Na_2S{\cdot}9H_2O$ was added and mixed, and unless indicated 10 ml of media was dispensed into tubes under a stream of O_2-free nitrogen.

Escherichia coli BL21 (DE3) CodonPlus was purchased from Novagen. Nco I, Xho I, T_4DNA ligase, DNA polymerase, isopropyl-β-D-thiogalactopyranoside (IPTG) and kanamycin were purchased from Takara (Dalian, China). RNase, *p*-nitrophenyl-acetate (*p*-NPC_2), *p*-nitrophenyl-butyrate (*p*-NPC_4), *p*-nitrophenyl-caprylate (*p*-NPC_8), *p*-nitrophenyl-caprate (*p*-NPC_{10}), p-nitrophenyl-laurate (*p*-NPC_{12}), *p*-nitrophenyl-myristate (*p*-NPC_{14}) and *p*-nitrophenyl-palmitate (*p*-NPC_{16}) were purchased from Sigma (St. Louis, USA). The other chemicals used were of the highest grade commercially available.

2.2. Identification and sequence analysis of FnL

The putative bacterial lipase encoded by Fond_1333 (GeneID: 5451971) was found from the genome sequence of *F. nodosum* Rt17-B1. Lipase and esterase sequences for comparative study were retrieved from protein and nucleotide databases on the NCBI Entrez server at http://www.ncbi.nlm.nih.gov/Entrez/. Sequence similarity searches were performed using BLAST at http://blast.ncbi.nlm.nih.gov/Blast.cgi. Phylogenetic trees were constructed using the neighbor-joining method with 1000 bootstrap replications implemented the phylogeny package MEGA4 [16].

2.3. Cloning, expression and purification of the lipase gene in E. coli

The gene was PCR amplified with primers up (5′-CATG CCATGGCTATGTATTATAACAACG-3′) and down (5′-CCGCTCGAG TTATTCTCCAAAAAAG-3′) (Nco I and Xho I sites underlined).

The PCR product was ligated into the vector pET-28a, and transformed into *E. coli* BL21 (DE3) CodonPlus for lipase gene expression, in which the gene is under the control of the T7 promoter and inducible with IPTG. Cells were harvested by centrifugation at 5000 rpm for 20 min. Cell pellets (corresponding to 1 g of dry weight) were re-suspended in 8 ml of 50 mM Tris–HCl pH 8.0 and disrupted by ultrasonic treatment for 5 min in 3 s on/5 s off cycles, on ice. The mixture was centrifuged for 20 min at 8000 rpm at 4 °C. SDS-PAGE analysis of the resulting supernatant and pellet revealed that the recombinant protein remained insoluble in the pellet. The insoluble fraction was suspended in 50 mM phosphate buffer (pH 8.0) and mixed thoroughly. After incubation of the suspension at 60 °C for 20 min, the mixture was centrifuged at 12,000 rpm for 30 min at 4 °C. SDS-PAGE analysis indicated that the recombinant protein was extracted and dissolved in the supernatant, which was applied to a Q-Sepharose Fast Flow column (GE Healthcare Bio-Sciences) that had previously been equilibrated with 50 mM phosphate buffer (pH 8.0). The column was washed with the same buffer and the protein was eluted with a linear gradient of 50 mM phosphate buffer (pH 8.0) and the same buffer containing 1.0 M NaCl at a flow rate of 1.0 ml min^{-1}. Eluting Proteins were monitored at 280 nm and collected in 1-ml fractions in which lipase activity was detected by *p*-NPC_8 assays. The fractions containing lipase activity were pooled and analyzed by 12% SDS-PAGE.

2.4. Mutagenesis

Mutants Ser119Ala, Asp260Asn and His282Asn were generated by whole-plasmid PCR with the following primers: 5′-TGCTC-ACGCCATGGGTGGAATTCTT-3′ and 5′-CCACCCATGGCGTGAGCAT-ATAT-3′, 5′-CTCAAAATAACGGGATGGTACCACT-3′ and 5′-CCATCCC-GTTATTTTGAGTAAAATCGG-3′, 5′-GGATTTGACAACGCAGACTTAG-CCAT-3′ and 5′-GTCTGCGTTGTCAAATCCTTCAAATAC-3′, respectively (modified codons underlined).

2.5. Enzyme and protein assays

Lipase activity was assayed by measuring the amount of *p*-nitrophenol formed from *p*-NPC_8 [17]. One unit of enzyme activity corresponds to the liberation of 1 μmol of *p*-nitrophenyl per minute ($\varepsilon_{420nm} = 0.016\ \mu M^{-1}$). The protein concentration in each sample was estimated by the method of Bradford [18].

Lipase activity was also detected by titrating the free fatty acids released by the hydrolysis of triglycerides and olive oil [19], using a substrates emulsion prepared by emulsifying 5 ml of olive oil in 20 ml of 4% (w/v) polyvinyl alcohol (PVA) (Sigma) solution. Each reaction system, which totalizes 3 ml, contained 2.55 ml of 50 mM phosphate buffer (pH 8.0), 250 μl of olive oil emulsion and 200 μl

of enzyme solution (0.6 mg/ml). The mixtures were incubated for 10 min at 65 °C with shaking. Fatty acids released during incubation were determined by titration with phenolphthalein standardized with 10 mM NaOH. One unit was defined as the amount of enzyme liberating 1 μmol of fatty acid per minute.

2.6. Characterization of FnL

2.6.1. Kinetic assay

Substrate specificity was determined using a variety of *p*-NP esters (*p*-NPC_2, *p*-NPC_4, *p*-NPC_8, *p*-NPC_{10}, *p*-NPC_{12}, *p*-NPC_{14} and *p*-NPC_{16}) and triacylglycerols (tributyrin, tricaprion, tricaprylin, tricaprin, trilaurin, trimyristin, tripalmitin and olive oil). Effects of different *p*-NP esters on the reaction rate were assayed spectrophotometrically at 60 °C in 50 mM phosphate buffer (pH 8.0). The Michaelis–Menten constant (K_m) and the maximum velocity (V_{max}) for each substrate under these conditions were calculated from Lineweaver–Burk Plots.

2.6.2. Effect of temperature on lipase activity

The effect of temperature on the lipase activity was measured, and the optimum temperature identified, in assays at pH 8.0 with 50 mM phosphate buffer and *p*-NPC_8 as a substrate at temperatures ranging from 40 to 75 °C. For stability determinations, the enzyme was preincubated at various temperatures (60, 65 and 70 °C) in 50 mM phosphate buffer (pH 8.0) for different periods and then assayed for residual activity.

2.6.3. Effect of pH on lipase activity

The effect of pH on the lipase activity was measured, and the optimum pH identified, in assays at 60 °C using *p*-NPC_8 as a substrate with pH ranging from 7.0 to 10.0. The buffers used contained 40 mM of each of acetic acid, N-[2-Hydroxyerhyl] piperazine-N′-ethane-sulfonic acid (HEPES), N-[Tris (hydroxymethyl) methyl]-3-aminopropanesulfonic acid sodium salt (TAPS), N-cyclohexyl-3-aminopropanesulfonic acid (CAPS) and 2-morpholinoethanesulfonic acid (MES) [20]. The pH was adjusted with 1N HCl or 1N NaOH at 60 °C.

2.6.4. Effects of metal ions, EDTA, PMSF and organic solvents on lipase activity

Various effectors, including 1 or 10 mM metal ions (Na^+, Mg^{2+}, Ca^{2+}, Zn^{2+}, Co^{2+}, Cu^{2+}, Ni^{2+}, and Mn^{2+}), 5 or 20% (v/v) organic solvents (methanol, ethanol, propanol, acetone, dimethyl sulfoxide and N,N-dimethylformamide) and 5 or 10 mM enzyme inhibitors (EDTA and PMSF) were added to the enzyme solution (1 mg/ml) and incubated at 37 °C for 30 min. Residual activity was determined by measuring the enzyme activity following the incubations using *p*-NPC_8 as a substrate at 60 °C in 50 mM phosphate buffer (pH 8.0).

2.7. Structural modeling, MD calculations and docking analysis

Since there are no close structural homologues of FnL, modeling was based on threading using the 3D-structural threading program Phyre [21,22]. A sequence search by fold recognition as implemented in the Phyre server, which is a well-established and successful annotation technique to predict the remote homology modeling from the known structures, is used to build model. Ten homology models were found. Their quality was assessed by using the 3D Profile of Insight II [23]. The top score, a serine hydrolase (PDB code 1J1I) from *Janthinobacterium* sp. strain J3, was selected as a template. The model was completed by addition of all hydrogen atoms and underwent energy minimization followed by MD simulation in explicit solvent with the sander module of the Amber 9 package [24], using PARM03 force field [25]. The protein was solvated using a box of TIP3P water molecules extending at least 10 Å away from the boundary of any protein atoms. Thus the structure was solvated in a box of 35858 TIP3P water molecules. An appropriate number of counterions were added to neutralize the system. The particle mesh Ewald (PME) method was employed to calculate the long-range electrostatics interactions. The system was gradually heated from 0 to 343 K in 15 ps with three intervals and then equilibrated for 25 ps at 343 K, followed by a data collection run, giving a total simulation time of 1000 ps at 343 K. The nonbonded cutoff was set to 10.0 Å and the nonbonded pairs were updated every 25 steps. The SHAKE method [26] was applied to constrain all covalent bonds involving hydrogen atoms. An integration time step of the MD calculations was 2 fs. The conformation with the lowest energy was chosen as the final model. This model was further checked by the 3D module of Insight II [23] and PROCHECK [27]. The 3D structures of the substrates were built through the Insight II/Builder program. Docking experiments was used AutoDock4.0 program [28], which calculates enzyme–ligand interaction energies over a grid, which size was set to be $126 \times 126 \times 126$ and the grid space was the default value of 0.375 Å.

3. Results and discussion

3.1. Identification of a new subfamily of bacterial lipases

In the genome sequence of *F. nodosum* Rt17-B1, a gene (Fond_1333) coding for a putative bacterial lipase composed of 302 amino acids residues was found. The amino acid sequence includes Ser119-Asp260-His282, a catalytic triad that is highly conserved in lipolytic enzymes of the α/β hydrolase superfamily. In addition, it has a pentapeptide consensus sequence, Ala-Xaa-Ser-Xaa-Gly (where Xaa stands for any amino acid), typical for lipolytic enzymes. A BLAST search of GenBank revealed similarities between FnL and four other proteins: a hypothetical protein from *Thermosipho melanesiensis* (41% identity), a hypothetical protein from *Thermotoga petrophila* (31% identity), a putative esterase from *Thermotoga* sp. RQ2 (31% identity), and a putative esterase from *Thermotoga maritime* (31% identity). These four proteins were identified from whole-genome sequences of bacteria but none of them have been characterized to date. Alignment of FnL, its four homologues and lipases from *Bacillus* sp. Tosh, *Vibrio cholerae*, *Pseudomonas* sp. KWI-56 and *Pseudomonas aeruginosa* indicated that the residues of the catalytic triad were highly conserved (Fig. 1). To confirm the predictions of the catalytic triad, amino acid residues of the catalytic triad were substituted by site-directed mutagenesis. Mutants Ser119Ala, Asp260Asn and His282Asn were generated by whole-plasmid PCR. None of the mutants had any detectable activity, confirming the importance of these three residues for the activity of FnL (Supplementary Table 1).

FnL was classified by constructing a phylogenetic tree for FnL, its homologues and other lipases based on the classification previously reported by Jaeger and colleagues. For the phylogenetic analysis, 36 bacterial lipolytic enzymes representing eight different families were selected. As shown in Fig. 2, FnL and the four homologues belong to family I, but they cannot be grouped in any of the known subfamilies of family I. Therefore, we suggest that they are members of a new subfamily within family I of bacterial lipases, designated as family I.8.

One important feature of lipases in this new subfamily is their origin, since all of them are from anaerobic thermophiles/hyperthermophiles of the order Thermotogales, with optimum temperatures between 70 and 82 °C. Thermotogales are the most extremely thermophilic eubacteria currently known and represent the deepest phylogenetic branch within the bacteria [15]. As mentioned above, no lipases have been previously cloned and they have not been classified into any bacterial lipase family since

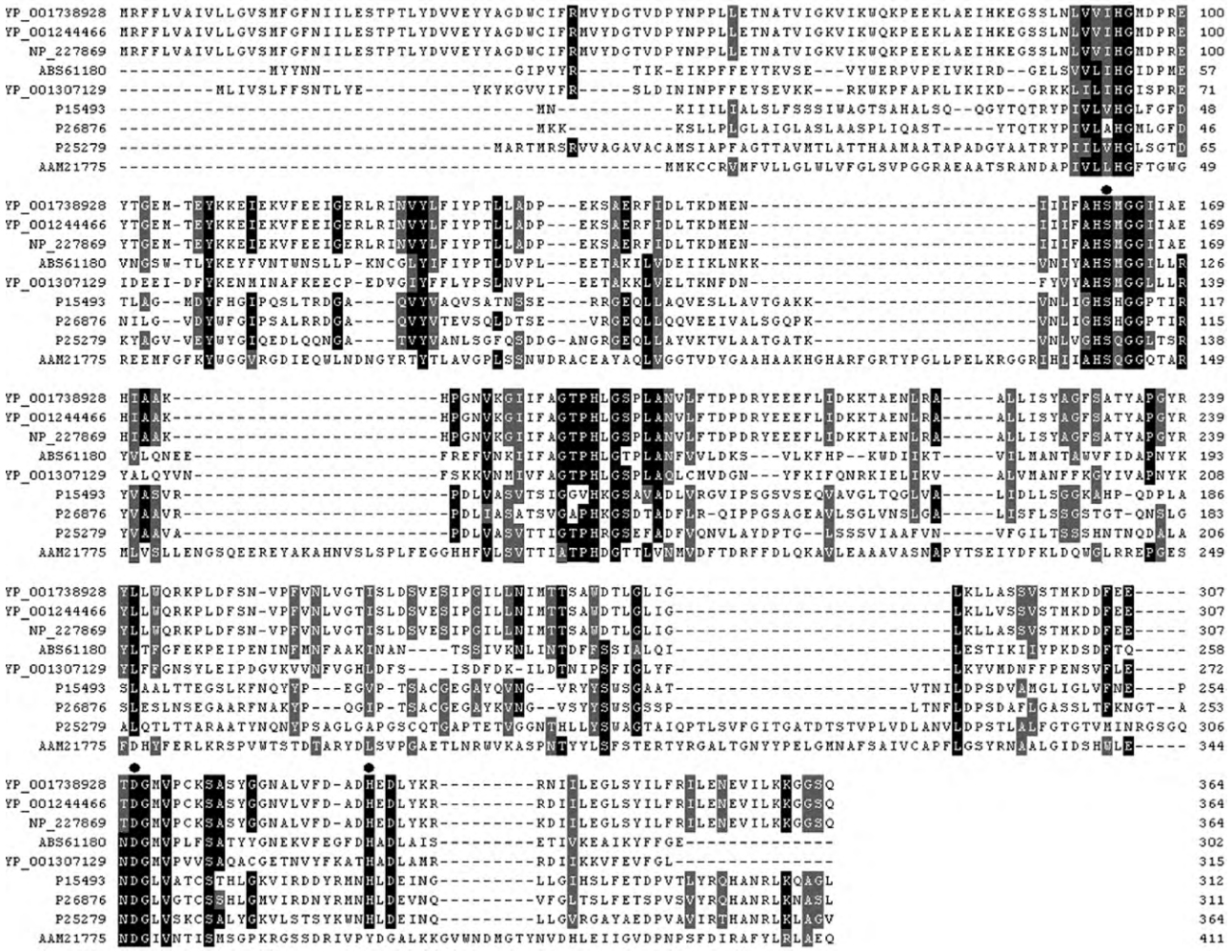

Fig. 1. Multiple amino acid sequence alignment of FnL, its homologues and other lipases. The accession numbers of the aligned sequences are for the following organisms: ABS61180, conserved hypothetical protein from *F. nodosum* Rt17-B1; YP_001738928, putative esterase from *Thermotoga* sp. RQ2; NP_227869, putative esterase from *Thermotoga maritime* MSB8; YP_001307129, hypothetical protein from *T. melanesiensis* BI429; YP_001244466, hypothetical protein from *T. petrophila* RKU-1; AAM21775, lipase (LipA) from *Bacillus* sp. Tosh; P15493, triacylglycerol lipase from *V. cholerae*; P25279, triacylglycerol lipase from *Pseudomonas* sp. KWI-56; P26876, triacylglycerol lipase from *Pseudomonas aeruginosa*. The accession numbers are indicated to the left of the amino acid sequences. Identical residues are indicated by a dark grey background. Symbols: ● amino acids forming a catalytic triad.

their cognate genes have not been previously reported [14]. Hence, the identification of this new subfamily extends the diversity of known bacterial lipases, especially thermophilic lipases, and distinguishes a new source of themophilic lipases. Another feature of the new subfamily is the active site pentapeptide sequence. All lipases in family I.8 have the active site pentapeptide AXSXG, in which Ala replaces the first Gly of the active site pentapeptide GXSXG found in most bacterial lipases. Interestingly, this AXSXG active site pentapeptide sequence is also found in thermophilic lipases belonging to family I.5 such as lipases from *B. thermocatenulatus* I [7], *B. stearothermophilus* L1 [8], *G. thermoleovorans* ID-1 [9], *G. stearothermophilus* P1 [10], *G. thermoleovorans* Toshki [11], *Geobacillus* sp. T1 [12], and *G. thermoleovorans* CCR11 [13]. Hence, the AXSXG active site pentapeptide sequence may be a signature sequence for thermophilic lipases.

3.2. Cloning, expression and purification of FnL

Bacteria transformed with the expression vector pET-FnL and induced with IPTG abundantly expressed the recombinant protein. FnL remained insoluble and sedimented when ultrasonicated extracts were centrifuged, according to SDS-PAGE analysis. A solubilization procedure was then applied to the insoluble fraction to extract the recombinant protein from the cells, and subsequent ion exchange chromatography step led to the purification of FnL with a recovery of 52.5% (from the solubilized quantity) and a purification factor of 1.75. The homogeneity of the purified protein was verified by SDS-PAGE, which showed a single band corresponding to purified FnL (Fig. 3). The specific activity of FnL was 52,000 U/mg using *p*-NPC_8 as a substrate in assays at 70 °C and pH 8.0.

3.3. Substrate specificity

The substrate specificity of the enzyme was initially assayed using *p*-NP esters with acyl chains of various lengths at 60 °C (Table 1). It proved to have higher activity towards medium chain length fatty acids (C_8–C_{12}) than either short- or long-chain fatty acids. The catalytic efficiency toward *p*-NPC_{10}, which was the best substrate for FnL, was approximately 180-fold higher than toward *p*-NPC_2. Moreover, when acyl chain lengths were less than 10, its k_{cat} values increased, while K_m values decreased with increasing acyl chain length. In contrast, when acyl chain lengths were in the range of 12–16, the k_{cat} values decreased, whereas K_m values remained constant with increasing acyl chain length. Further titration tests using triglycerides as substrates revealed that FnL has a wide range of substrates from C_4 to C_{16} with the highest activ-

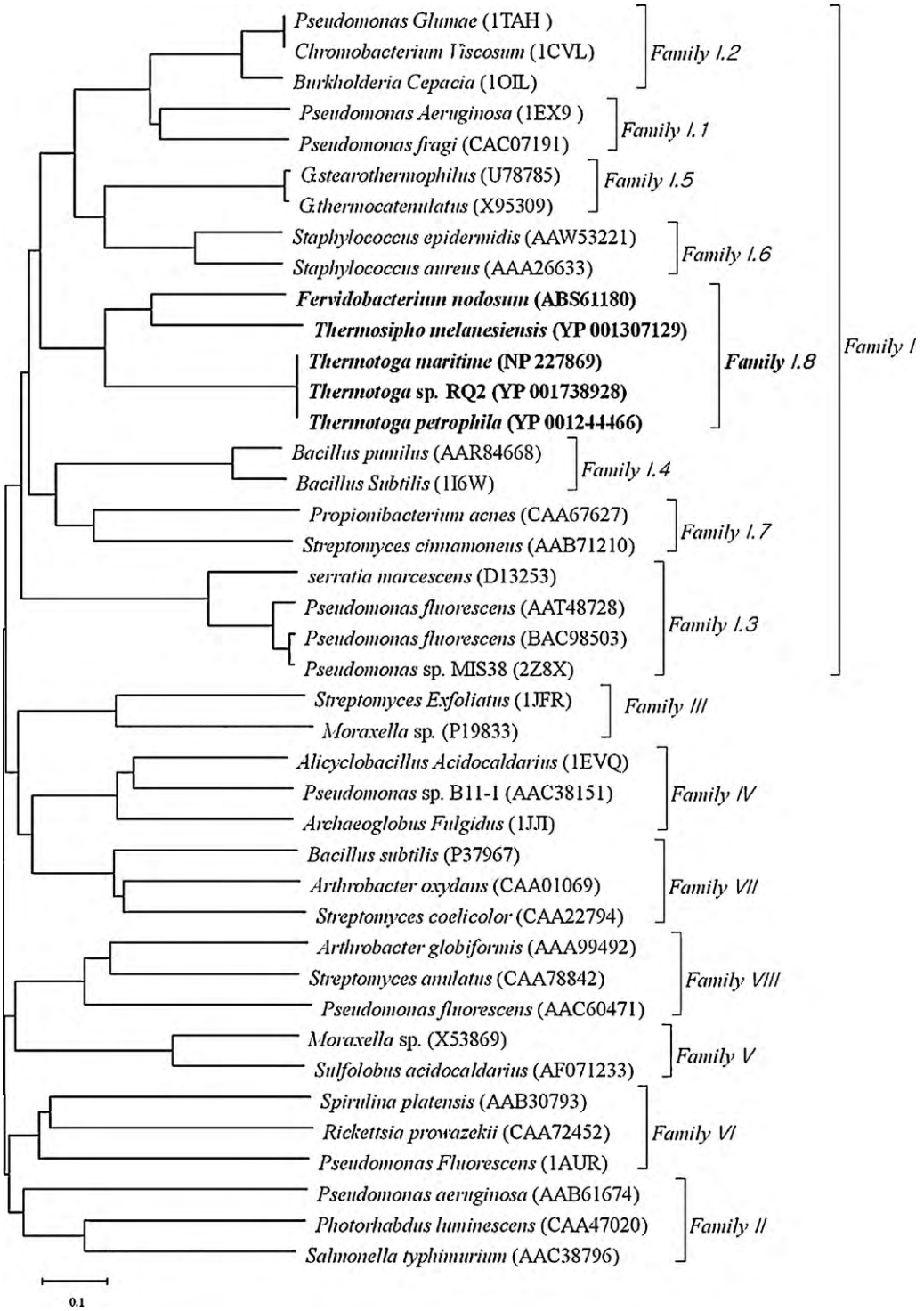

Fig. 2. Phylogenetic analysis of FnL, its homologues and other lipases. The units at the bottom of the tree indicate numbers of substitution events.

Table 1
Kinetic parameters and binding free energies for FnL with *p*-NP esters ranging from *p*-NPC_2 to *p*-NPC_{16}.

Substrate (*p*-Nitrophenyl ester)	K_m (μM)	k_{cat} (s^{-1})	k_{cat}/K_m (s^{-1} mM^{-1})	$\Delta G_{binding}$
p-NPC_2	163 ± 23.6	19.1 ± 1.78	120	−3.58
p-NPC_4	122 ± 19.0	36.4 ± 1.53	299	−3.94
p-NPC_8	9.34 ± 0.06	53.4 ± 0.22	5720	−4.22
p-NPC_{10}	3.93 ± 0.14	88.5 ± 2.55	22,500	−5.07
p-NPC_{12}	4.90 ± 1.36	42.6 ± 4.99	8690	−4.22
p-NPC_{14}	5.39 ± 0.19	30.5 ± 0.72	5890	−4.17
p-NPC_{16}	5.49 ± 1.39	27.8 ± 3.22	5070	−4.03

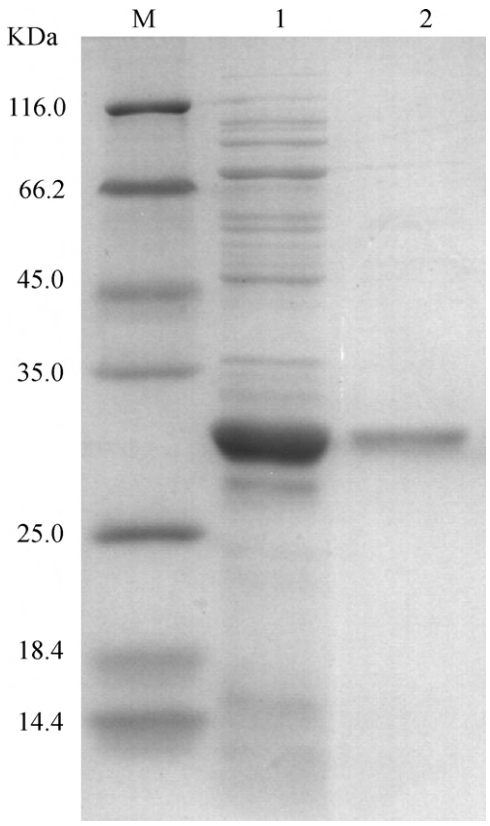

Fig. 3. Purification of FnL. Lane M, molecular mass marker; lane 1, heat-treated crude extract; lane 2, FnL after Q-Sepharose Fast-Flow purification.

ity toward tributyrin (C_4). The specific activity was found to be ca. 25,000 U/g using olive oil emulsion as substrate at pH 8.0 and 65 °C (Fig. 4A). The preferences of FnL toward tributyrin (C_4) and *p*-NP caprate (C_{10}) differ from those of other described thermophilic lipases in family I.5. For example, the thermophilic enzyme from *G. thermoleovorans* ID-1 showed maximum activity toward tricaproin (C_6) and *p*-NP caproate (C_6) [8], that from *G. stearothermophilus* P1 toward tricaprylin (C_8) and *p*-NP caprate (C_{10}) [9], that from *B. stearothermophilus* L1 toward tripropionin (C_3) and *p*-NP caprylate (C_8) [7], and that from *B. thermocatenulatus* I toward tributyrin (C_4) and *p*-NP butyrate (C_4) [6].

3.4. Effects of temperature and pH on lipase activity and stability

The effect of temperature on the activity of the lipase was determined using *p*-NPC_8 as a substrate at pH 8.0 in the temperature range 40–75 °C. FnL was active across this temperature range, with maximal activity at 70 °C and 45% of maximal activity at 40 °C (Fig. 4B). To test the thermostability of FnL, the enzyme was incubated at various temperatures, and the residual activities were assayed. As can be seen in Fig. 4C, the enzyme remained stable at temperatures below 70 °C and could be incubated for at least 50 h without an obvious loss of activity at 60 °C. Even at 70 °C, the optimal temperature for activity, it had a half-life of about 8 h. Above 70 °C, the lipase activity decreased rapidly, since the enzyme retained just 30% residual activity when incubated for about 10 min at 75 °C. Hence, it was less stable than the lipase from *G. thermoleovorans* Toshki, which can reportedly retain 30% residual activity when incubated for 1 h at 100 °C. However, the thermostability of FnL was still very high, since it appears to be much more stable than other lipases of family I.5, such as those from *B. thermocatenulatus* I [7], *B. stearothermophilus* L1 [8], *G. thermoleovorans* ID-1 [9], *G. stearothermophilus* P1 [10] and *Geobacillus* sp. T1 [12], which reportedly have half-lives ranged from 0.5 h to 7.6 h at the temperatures around 60 °C.

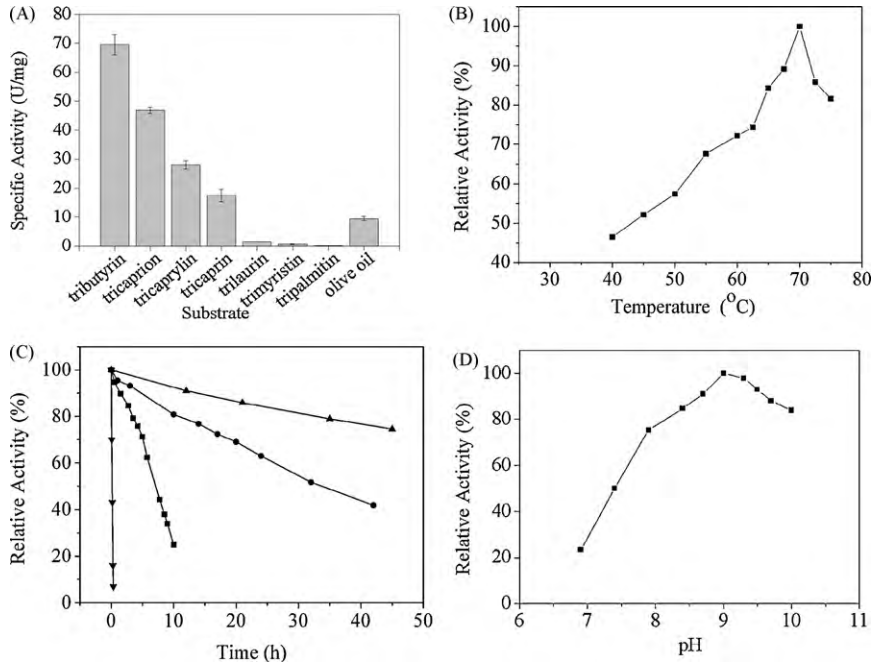

Fig. 4. (A) Substrate specificity of FnL toward triacylglycerols with different acyl chain lengths (C_4–C_{16}). The lipase activity was determined by titration with phenolphthalein standardized with 10 mM NaOH at pH 8.0 and 65 °C. (B) Effect of temperature on enzyme activity. The activities were determined by assays with *p*-NPC_8 as substrate in the temperature range 40–75 °C. 100% relative activity corresponds to 52,000 U/mg FnL. (C) Effect of temperature on enzyme stability. The activities were determined by assays with *p*-NPC_8 as substrate following incubation of the enzyme at 60 °C (▲), 65 °C (●), 70 °C (■) and 75 ° (▼) for the indicated times. (D) Effect of pH on enzyme activity. The activities were determined by assays with *p*-NPC_8 as substrate at 60 °C at the indicated pH. The buffers used contained 40 mM acetic acid, HEPES, TAPS, CAPS and MES. 100% relative activity corresponds to 38,000 U/mg FnL.

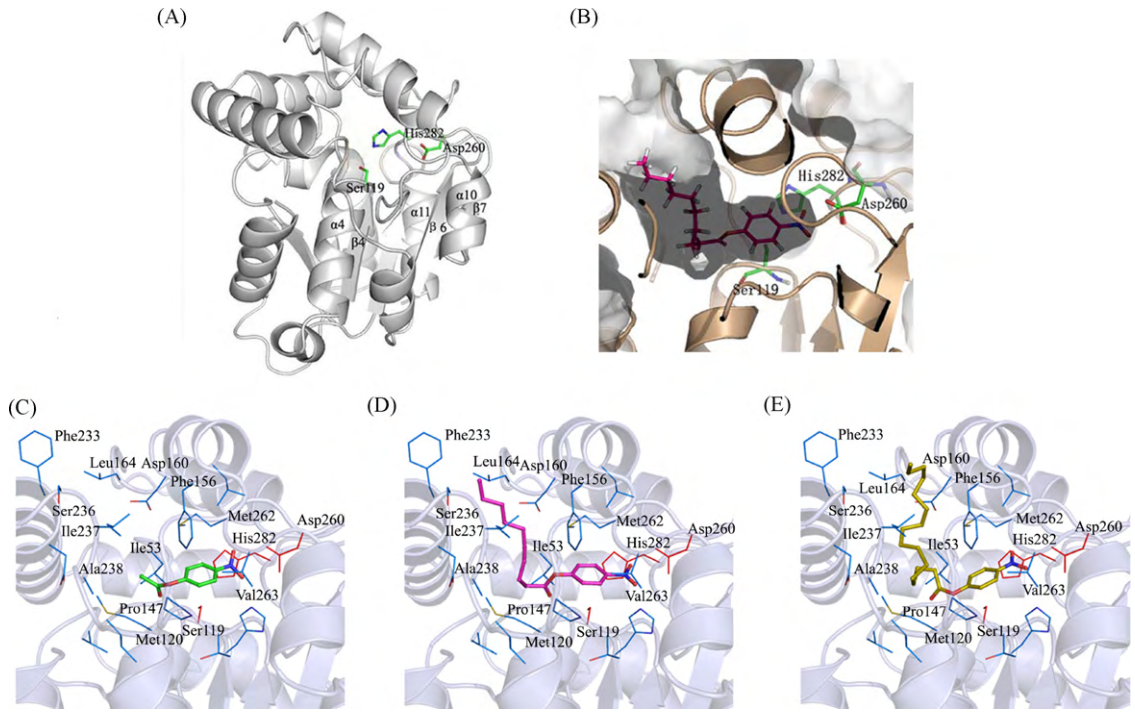

Fig. 5. (A) Overall structure of FnL. The central β-sheet and surrounding α-helixes are shown in grey with α3, α10, α11, β4, β6 and β7 indicated. Residues of the active site triad (Ser119, His282 and Asp260) are indicated. (B) The surface of FnL model showing the central cavity and the bound *p*-NPC_{10} molecule near the active site. The *p*-NPC_{10} is shown in magenta, and the location of the catalytic triad is marked in green stick. The FnL structure is shown in ribbon representation and is colored wheat. (C) A zooming view of the active site and the binding pocket of FnL in the docking model. The shortest chain substrate *p*-NPC_2 near the active site is marked in green strick. The catalytic trial and residues involved in the substrate binding are indicated and colored in red and blue, respectively. (D) A zooming view showing the docking model with the optimum substrate *p*-NPC_{10}. (E) A zooming view showing the docking model with the longest chain substrate *p*-NPC_{16}.

FnL is only active under alkaline conditions. It exhibited >80% of maximal activity in the pH range of 8.0–10.0, and highest activity at a pH of approximately 9.0 (Fig. 4D).

3.5. Effects of organic solvents on lipase stability

Another outstanding property of FnL is its maintenance of activity in the presence of various organic solvents. This is a key feature for many potential industrial applications, but most enzymes (including lipases) are not stable in the presence of organic solvents, especially polar organic solvents which are highly toxic to most enzymes, therefore few organic solvent-tolerant bacterial lipases are known as yet [29–31]. We found that exposure of FnL to various organic solvents at concentrations of 5 or 20% (v/v) for 30 min at 37 °C had little effect on its activity, showing that it is stable to all tested organic solvents (Table 2). Indeed, addition of 5 or 20% (v/v) of several polar organic solvents (including propanol, acetone, DMSO and DMF) resulted in 9–56% increases in its activity in comparison with control (organic solvent-free) activity. The stability and activation effects of FnL in the presence of water–organic solvent mixture suggest that this enzyme can resist denaturation by organic solvents and form multiple hydrogen bonds with water, providing the structural flexibility and conformational mobility required for optimal catalysis [32]. Therefore, FnL has potential utility in organic synthesis and related applications.

3.6. Effects of metal ions, EDTA and PMSF on lipase activity

As shown in Table 2, significant inhibition was observed with 1 mM Zn^{2+} and Cu^{2+} (residual activity, 51 and 73%, respectively), and the inhibition increased as the concentration of the ions increased. In contrast, 1 mM Mg^{2+}, Ca^{2+}, Na^{+}, Ni^{2+} and Co^{2+} slightly activated the activity (by 6–24%). When these ions were assayed at a concentration of 10 mM, activation was also detected in the presence of Mg^{2+}, Ca^{2+} and Na^{+}, whereas Ni^{2+} showed inhibitory effects (residual activity, 76%). In addition, the presence of 5 or 10 mM EDTA caused no significant reduction in the enzyme's activity, suggesting that metal ions, especially Ca^{2+} are not essential for its enzyme activity.

Lipases are generally serine hydrolases, in which serine is an essential residue for catalytic activity. The addition of 5 or 10 mM of the serine hydrolase inhibitor PMSF inhibited FnL's lipase activity (residual activity, 13 and 5%, respectively) (Table 2), indicating that it is also a serine hydrolase.

Table 2
Effects of metal ions, inhibitor and organic solvents on the enzyme activity of FnL.

Additives	Relative activity (%)	
Control wild type FnL	100 ± 1.4	100 ± 1.2
Metal ions	1 mM	10 mM
$MgCl_2$	114 ± 1.8	129 ± 1.1
NaCl	114 ± 3.5	114 ± 2.6
$NiCl_2$	112 ± 2.2	76.4 ± 2.2
$MnCl_2$	104 ± 1.7	94.0 ± 1.1
$CaCl_2$	106 ± 1.5	122 ± 2.1
$ZnCl_2$	51.8 ± 0.9	47.5 ± 1.6
$CoCl_2$	124 ± 4.2	100 ± 3.7
$CuCl_2$	73.8 ± 4.3	5.1 ± 0.2
Inhibitors	5 mM	10 mM
PMSF	13.4 ± 0.7	5.1 ± 1.6
EDTA	94.4 ± 0.8	96.5 ± 4.8
Organic Solvents	5% (v/w)	20% (v/w)
Methanol	99.9 ± 0.0	101 ± 0.4
Ethanol	109 ± 3.3	101 ± 1.0
Propanol	156 ± 2.3	110 ± 0.6
Acetone	113 ± 1.2	127 ± 0.5
DMSO	120 ± 4.8	126 ± 2.8
DMF	135 ± 1.0	151 ± 2.3

Table 3
The total energy (E_{total}), van-der-Waals energy (E_{vdW}) and electrostatic energy (E_{ele}) between substrates (*p*-NPC_2, *p*-NPC_{10} and *p*-NPC_{16}) and individual residues ($E_{total} < -1.00$ kcal mol^{-1} listed in energy rank order).

p-NPC_2				*p*-NPC_{10}				*p*-NPC_{16}			
Residues	E_{vdW} (kcal mol^{-1})	E_{ele} (kcal mol^{-1})	E_{total} (kcal mol^{-1})	Residues	E_{vdW} (kcal mol^{-1})	E_{ele} (kcal mol^{-1})	E_{total} (kcal mol^{-1})	Residues	E_{vdW} (kcal mol^{-1})	E_{ele} (kcal mol^{-1})	E_{total} (kcal mol^{-1})
Gly52	−0.35	−0.66	−1.01	Gly52	−0.33	−0.67	−1.00	Thr146	−2.02	0.14	−1.88
Met120	−1.83	0.46	−1.37	Ile53	−4.08	0.02	−4.06	Leu164	−1.41	0.07	−1.34
Thr146	−1.78	0.02	−1.76	Met120	−2.98	0.73	−2.25	Asp232	−2.49	−0.12	−2.61
Phe156	−2.03	0.17	−1.86	Pro147	−1.82	−0.34	−2.16	Gly261	−0.61	−0.44	−1.05
Gly261	−0.61	−0.55	−1.16	Phe156	−4.98	0.11	−4.87				
Met262	−2.65	−0.49	−3.14	Asp160	−1.98	0.16	−1.82				
Val263	−1.33	−0.19	−1.52	Asp232	−2.02	−0.01	−2.03				
				Phe233	−1.98	−0.27	−2.25				
				Ser236	−1.52	−0.16	−1.68				
				Met262	−3.26	0.00	−3.26				
				Val263	−1.75	−0.13	−1.88				
Total	−10.6	−1.24	−11.8		−26.7	−0.56	−27.3		−6.53	−0.35	−6.88

3.7. Structural modeling

A model of FnL was constructed based on threading using Phyre [21,22]. The quality of the final model was analyzed by PROCHECK [26] and Profile-3D [24]. A Ramachandran plot obtained using the model (Supplementary Fig. 1) indicated that about 90% of the enzyme's residues were in the core and allowed regions. The overall self-compatibility score for the protein was 94.90; higher than the threshold of 50.91 accepted for a correct fold prediction, and close to the top possible score of 113.14, indicating that the model is reliable.

The model of FnL showed a large domain with an α/β hydrolase fold and a lid domain comprised of four α-helices. The α/β-hydrolase fold consists of a seven-central β-sheet and eight α-helixes. Catalytic residue Ser119 is located within a nucleophile elbow connecting strand β4 and helix α4, while catalytic residues Asp260 and His282 are located in loops between β6–α10 and β7–α11, respectively (Fig. 5A). The substrate *p*-NPC_{10} was docked into FnL as shown in Fig. 5B, and the putative substrate binding pocket was found to extend in a tunnel on both sides of Ser119.

As seen in Fig. 5C, D and E, the pocket provides a hydrophobic environment for the substrate and is lined by the residues Ile53, Met120, Ile123, Pro147, Phe156, Leu164, Met262, Val263, Ile237 and Ala238. To determine the key residues in the binding pocket, the interaction energies of *p*-NPC_2, *p*-NPC_{10} and *p*-NPC_{16} with FnL were calculated with Affinity program. Table 3 gives the interaction energies including the total energies, van-der-Waals, and the electrostatic energies; the residues within a sphere defined by 4.0 Å radius around substrates were recorded as well (Table 3). For the complex models, which were bound substrates *p*-NPC_2 and *p*-NPC_{10}, the van-der-Waals (vdW) energies are much larger than the electrostatic energies. It means that the interaction is mainly hydrophobic interaction. For instance, the complex of FnL and *p*-NPC_{10} has total interaction energy of −27.3 kcal mol^{-1}, the vdW energies and electrostatic energies are −26.7 and −0.56 kcal mol^{-1}, respectively. Moreover, only Met120 and Gly52 can form strong electrostatic interactions (hydrogen bonds) with the oxygen of *p*-NPC substrates. Their participation in ligand binding is important for anchoring the substrate, and the presence of these two residues is identified as oxynion hole. Furthermore, the edge-to-face interaction between Phe156 and substrates, and hydrophobic interactions between Met262, Val263 and substrates are significant for the substrate binding. In addition, residues Asp160, Asp232, Ser236, Pro147 and Phe233 have important contributions to the substrate binding of *p*-NPC_{10} by electrostatic interaction, hydrophobic interaction and aromatic interaction, respectively [33].

3.8. Docking analysis of substrate specificity

In order to understand more about the substrate specificity of FnL, seven substrates (*p*-NPC_2–*p*-NPC_{16}) were docked into FnL with AutoDock 4.0 program. The binding free energy ($\Delta G_{binding}$) of the complex has been calculated independently. As shown in Table 1, the $\Delta G_{binding}$ decreased in the beginning and then increased with the alkyl group extending from C_2 to C_{16}. The inflexion of $\Delta G_{binding}$ corresponds to the binding free energy between *p*-NPC_{10} and FnL, which is the lowest binding free energy (−5.07 kcal mol^{-1}) among the seven enzyme–substrate complexes. This profile is consistent with the profile of the K_m value and is contrary to the profile of the k_{cat} value for the experimental kinetic parameters (Table 1). This kind of behavior characterizes that FnL displayed the highest catalytic efficiency towards *p*-NPC_{10}. Compared with 3D model of seven complexes, the difference among these substrates lies in the various chain lengths (C_2–C_{16}) of the alkyl group. Theoretically, the longer alkyl group is a better electron donor than that of the short alkyl group, and thus they can make the carboxyl oxygen

center of the substrate slightly more negative, which makes formation of the negatively charged tetrahedral intermediate slightly easier [34–36]. It seems that the activity should increase with the extension of the substrate alkyl chain theoretically.

On the other hand, the complex models unambiguously map out the substrate binding pocket located in close proximity to the active site (Fig. 5C, D and E). As shown in Fig. 5, the shortest and longest substrates *p*-NPC_2 and *p*-NPC_{16} are placed in a similar position to *p*-NPC_{10}. However, the planes of an alkyl group prospectively formed some steric clashes between the *p*-NPC_{16} and the residues in active site pocket. As seen in Fig. 5B, the active site pocket seems to be most appropriate for an alkyl group with a 10–10 carbon chain. This discovery was further confirmed by calculating the binding free energy. The binding free energy between *p*-NPC_{16} and FnL was -4.03 kcal mol^{-1}, while *p*-NPC_{10} and FnL was -5.07 kcal mol^{-1}. This result implies that *p*-NPC_{16} cannot steadily bind with FnL as well as *p*-NPC_{10}. Therefore, these theoretical analyses can be used to explained the trend of K_m and k_{cat} values when acyl chain lengths were in a range of 10–16.

4. Conclusion

FnL, the first thermophilic lipase to be cloned from an anaerobic thermophilic bacterium, appears to represent a new subfamily of family I of bacterial lipases, annotated as family I.8. It has been characterized in terms of optimal temperature, optimal pH, thermostability, tolerance of organic solvents and substrate specificity. Moreover based on the constructed model, the substrate specificity was explained by analyses in the aspects of the binding free energy, spatial obstruction, and interactions between enzyme and substrate in the active site. Our findings extend our knowledge about properties and the diversity of thermophilic lipases. Moreover, the desirable characteristics of FnL, including high thermal activity, stability and tolerance of organic solvents make it good candidate for many industrial applications.

Acknowledgments

This work was supported by the High Technology Project of China (863 Program, 2006AA020202, and 2006AA020203), National Basic Research Program of China (973 Program, 2004CB719606).

Appendix A. Supplementary data

Supplementary data associated with this article can be found, in the online version, at doi:10.1016/j.molcatb.2010.03.007.

References

[1] K.E. Jaeger, B.W. Dijkstra, M.T. Reetz, Annu. Rev. Microbiol. 53 (1999) 315–351.
[2] J.L. Arpigny, K.E. Jaeger, Biochem. J. 343 (1999) 177–183.
[3] R. Gupta, N. Gupta, P. Rathi, Appl. Microbiol. Biotechnol. 64 (2004) 763–781.
[4] P. Fojan, P.H. Jonson, M.T.N. Petersen, S.B. Petersen, Biochimie 82 (2000) 1033–1041.
[5] M. Nardini, B.W. Dijkstra, Curr. Opin. Struct. Biol. 9 (1999) 732–737.
[6] C. Schmidt-Dannert, M. Luisa Rfia, H. Atomi, R.D. Schmid, Biochim. Biophys. Acta 1301 (1996) 105–114.
[7] H.K. Kim, S.Y. Park, J.K. Lee, T.K. Oh, Biosci. Biotechnol. Biochem. 62 (1998) 66–71.
[8] A.R. Cho, S.K. Yoo, E.J. Kim, FEMS Microbiol. Lett. 186 (2000) 235–238.
[9] S. Sinchaikul, B. Sookkheo, S. Phutrakul, F.M. Pan, S.T. Chen, Protein Expr. Purif. 22 (2001) 388–398.
[10] Y.R. Abdel-Fattah, A.A. Gaballa, Microbiol. Res. 163 (2008) 13–20.
[11] T.C. Leow, R.N.Z.R.A. Rahman, Extremophiles 11 (2007) 527–535.
[12] R. Quintana-Castro, P. Díaz, G. Valerio-Alfaro, H.S. García, R. Oliart-Ros, Mol. Biotechnol. 42 (2009) 75–83.
[13] M.A. Salameh, J. Wiegel, Adv. Appl. Microbiol. 61 (2007) 253–283.
[14] M.A. Salameh, J. Wiegel, Appl. Environ. Microbiol. 73 (2007) 7725–7731.
[15] B.K.C. Patel, H.W. Morgan, R.M. Daniel, Arch. Microbiol. 141 (1984) 63–69.
[16] K. Tamura, J. Dudley, M. Nei, S. Kumar, Mol. Biol. Evol. 24 (2007) 1596–1599.
[17] R.J. Gao, Y. Feng, K. Ishikawa, H. Ishida, S. Ando, Y. Kosugi, S.G. Cao, J. Mol. Catal. B: Enzym. 24–25 (2003) 1–8.
[18] M.M. Bradford, Anal. Biochem. 72 (1976) 248–254.
[19] S. Dharmsthiti, J. Pratuangdejkul, G.T. Theeragool, S. Luchai, J. Gen. Appl. Microbiol. 44 (1998) 139–145.
[20] T. Juhász, Z. Szeltner, L. Polgár, FEBS Lett. 580 (2006) 3493–3497.
[21] P.A. Bates, L.A. Kelley, R.M. MacCallum, M.J. Sternberg, Proteins 45 (2001) 39–46.
[22] L.A. Kelley, M.J.E. Sternberg, Nat. Protoc. 4 (2009) 363–371.
[23] R. Luthy, J.U. Bowie, D. Eisenberg, Nature 356 (1992) 83–85.
[24] D.A. Case, T.A. Darden, T.E. Cheatham III, C.L. Simmerling, J. Wang, R.E. Duke, R. Luo, K.M. Merz, D.A. Pearlman, M. Crowley, R.C. Walker, W. Zhang, B. Wang, S. Hayik, A. Roitberg, G. Seabra, K.F. Wong, F. Paesani, X. Wu, S. Brozell, V. Tsui, H. Gohlke, L. Yang, C. Tan, J. Mongan, V. Hornak, G. Cui, P. Beroza, D.H. Mathews, C. Schafmeister, W.S. Ross, P.A. Kollman, AMBER 9, University of California, San Francisco, 2006.
[25] P. Trodler, R.D. Schmid, J. Pleiss, BMC Struct. Biol. 9 (2009) 38.
[26] J.-P. Ryckaert, G. Ciccotti, H.J.C. Berendsen, J. Computat. Phys. 23 (1977) 327–341.
[27] R.A. Laskowski, M.W. MacArthur, D.S. Moss, J.M. Thornton, J. Appl. Cryst. 26 (1993) 283–291.
[28] H. Huey, G.M. Morris, A.J. Olson, D.H. Goodsell, J. Comput. Chem. 28 (2007) 1145–1152.
[29] C.J. Hun, R.N. Zaliha, A. Rahman, A.B. Salleh, M. Basri, Biochem. Eng. J. 15 (2003) 147–151.
[30] H. Ogino, H. Ishikawa, J. Biosci. Bioeng. 91 (2001) 109–116.
[31] G.A. Sellek, J.B. Chaudhuri, Enzyme Microbiol. Technol. 25 (1999) 471–482.
[32] A.M. Klibanov, Nature 409 (2001) 241–246.
[33] E.B. De Oliveira, C. Humeau, L. Chebil, E.R. Maia, F. Dehez, B. Maigret, M. Ghoul, J.M. Engasser, J. Mol. Catal. B: Enzym. 59 (2009) 96–105.
[34] D.H. Williams, E. Stephens, D.P. OBrien, M. Zhou, Angew. Chem. Int. Ed. 43 (2004) 6596–6616.
[35] M.A.J. Veld, L. Fransson, A.R.A. Palmans, E.W. Meijer, K. Hult, ChemBioChem 10 (2009) 1330–1334.
[36] M. Svedendahl, P. Carlqvist, C. Branneby, O. Allner, A. Frise, K. Hult, P. Berglund, T. Brinck, ChemBioChem 9 (2008) 2443–2451.